

Supplementary Materials for

**Activation of PDGFRA signaling contributes to filamin C–related  
arrhythmogenic cardiomyopathy**

Suet Nee Chen\*, Chi Keung Lam, Ying-Wooi Wan, Shanshan Gao, Olfat A. Malak,  
Shane Rui Zhao, Raffaella Lombardi, Amrut V. Ambardekar, Michael R. Bristow,  
Joseph Cleveland, Marta Gigli, Gianfranco Sinagra, Sharon Graw, Matthew R.G. Taylor,  
Joseph C. Wu\*, Luisa Mestroni\*

\*Corresponding author. Email: [suet.chen@cuanschutz.edu](mailto:suet.chen@cuanschutz.edu) (S.N.C.); [joewu@stanford.edu](mailto:joewu@stanford.edu) (J.C.W.);  
[luisa.mestroni@cuanschutz.edu](mailto:luisa.mestroni@cuanschutz.edu) (L.M.)

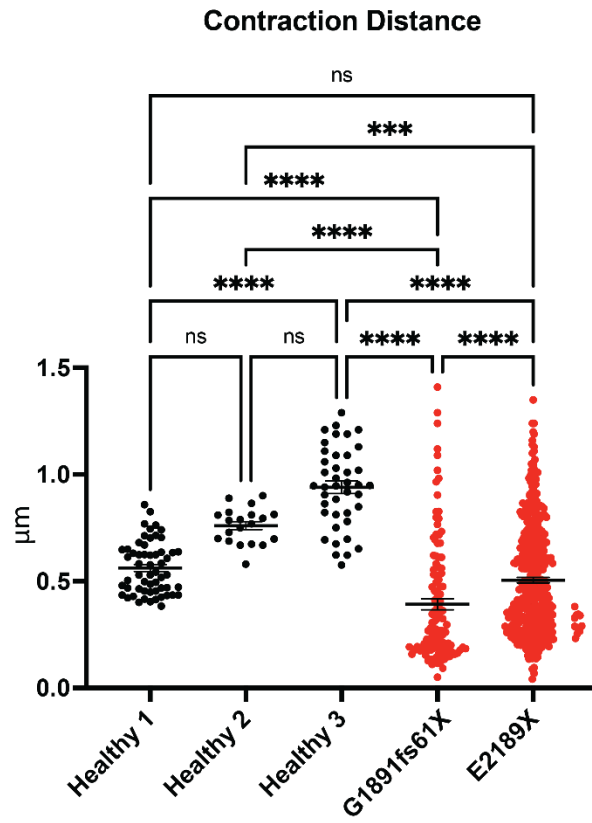
Published 23 February 2022, *Sci. Adv.* **8**, eabk0052 (2022)  
DOI: 10.1126/sciadv.abk0052

**This PDF file includes:**

Figs. S1 to S20  
Tables S1 to S3

## Supplementary Materials

### A



### B

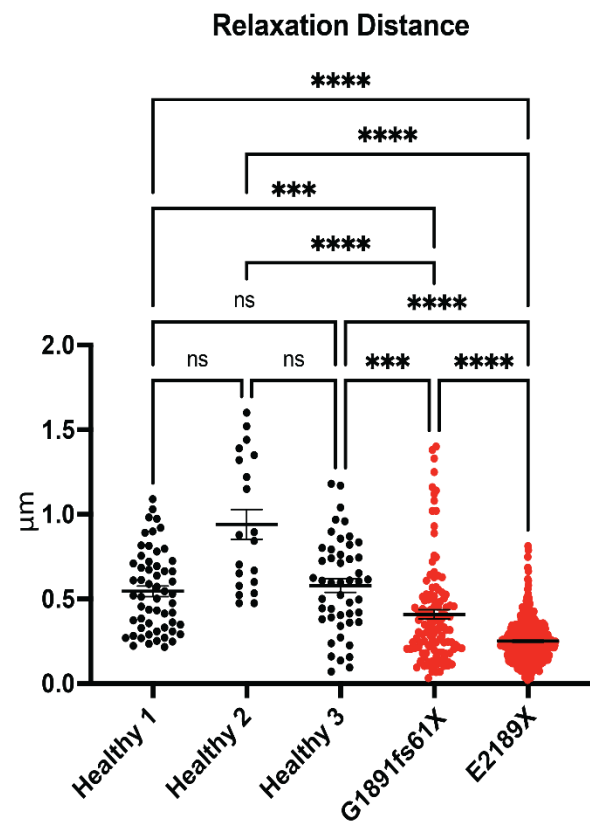
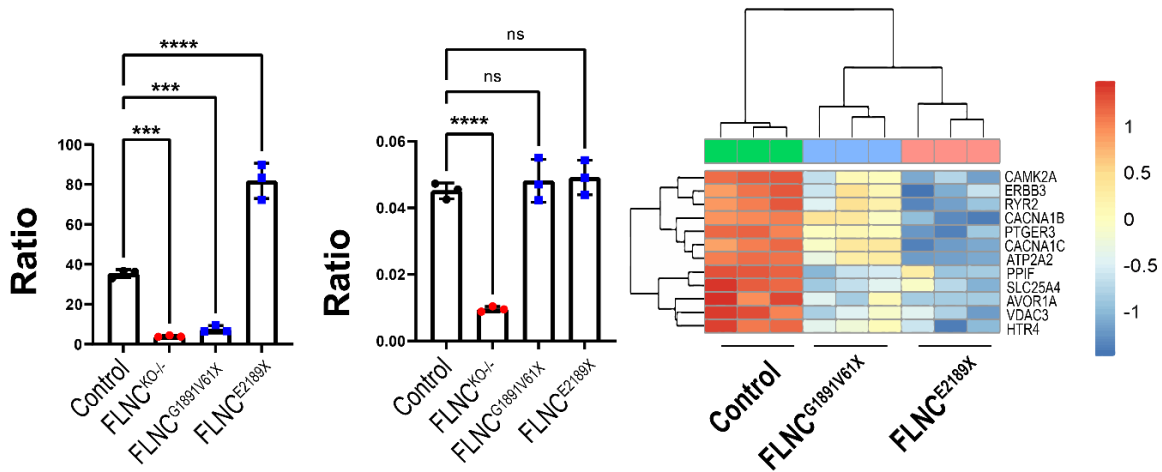
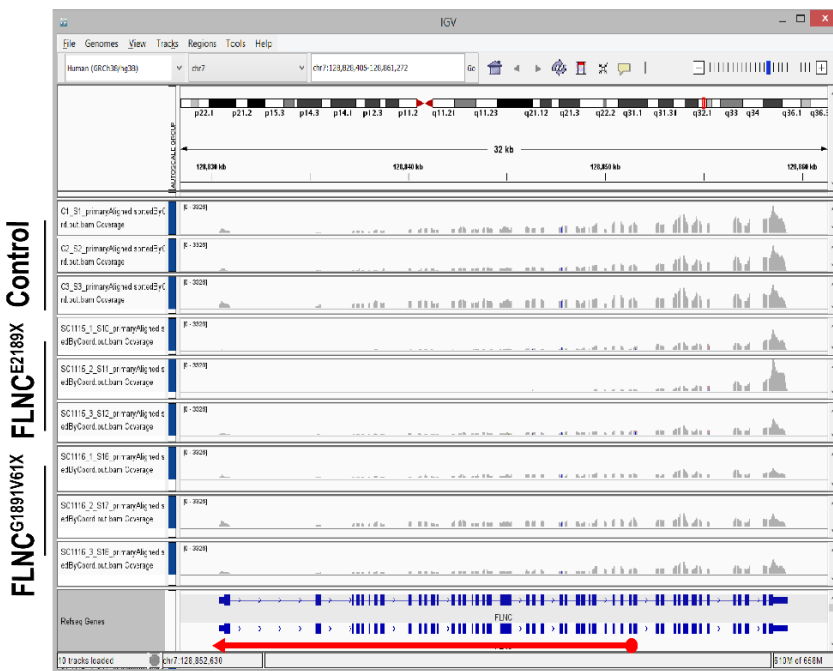


**Fig. S1. FLNC<sup>G1891Vfs61X</sup> and FLNC<sup>E2189X</sup> iPSC-CMs exhibited impaired contraction and relaxation distances.** n = 20 – 400 replicates from 2 different batches. ns: not significant, \*\*\* p-value < 0.005, \*\*\*\* p-value < 0.0001.

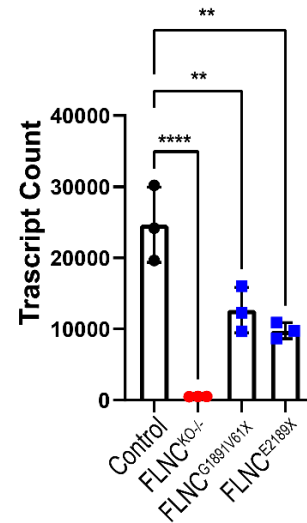
**A** *MYH7/MYH6*      **B** *TNNI3/TNNI1*      **C** KEGG Pathway: hsa04020 Calcium signaling pathway



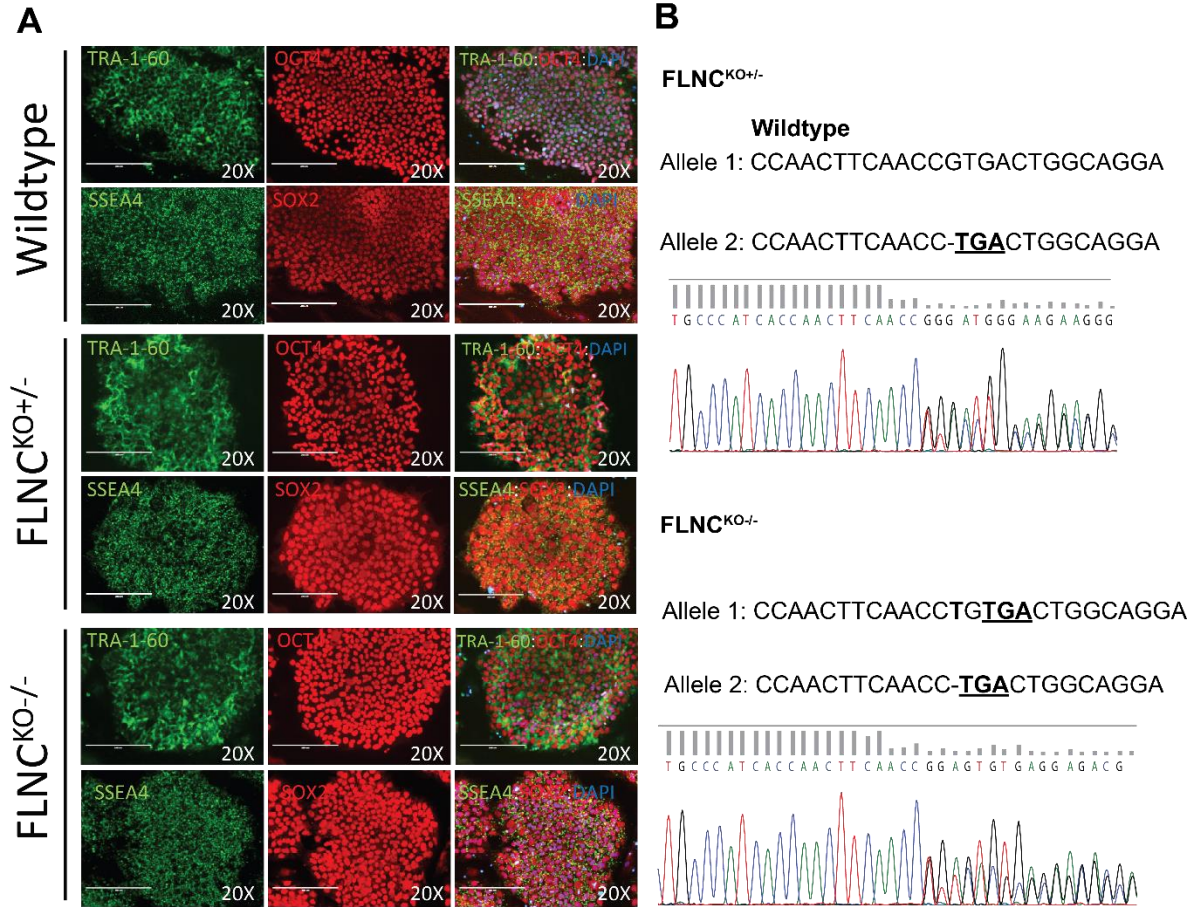
**D**



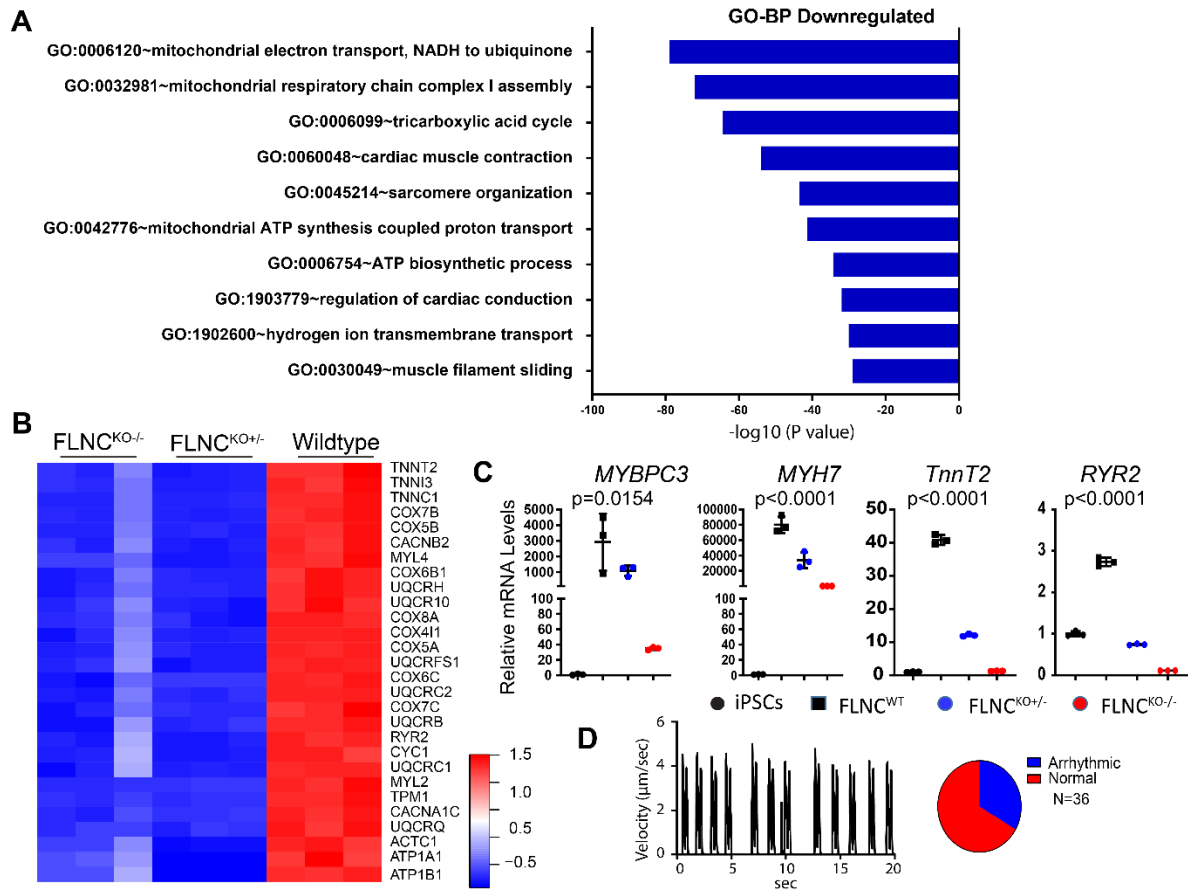
**E**



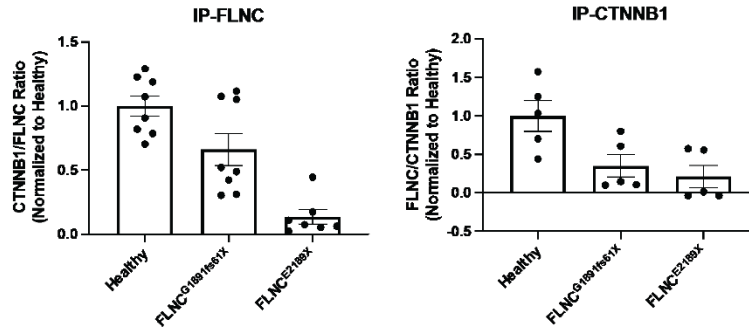
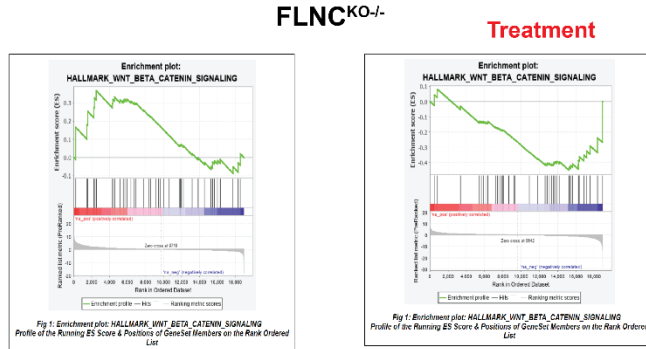
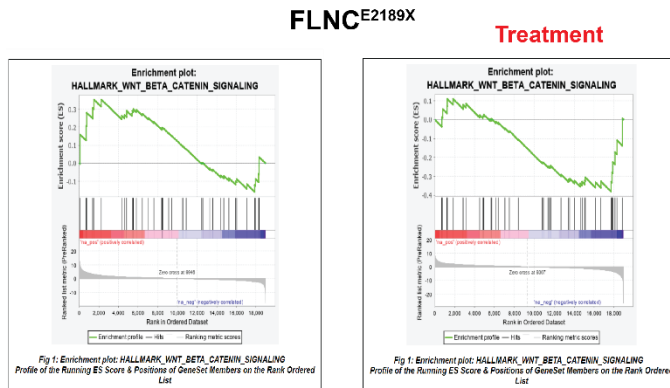
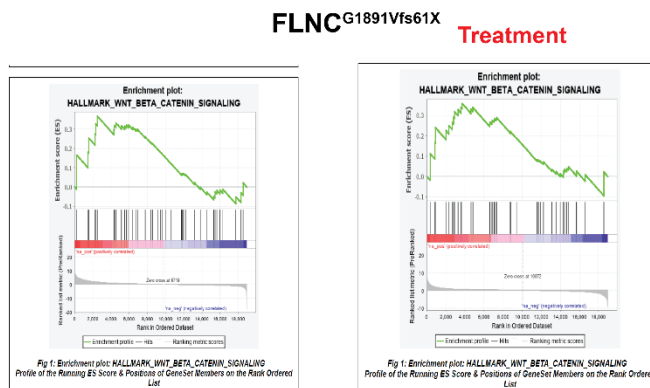
**Fig. S2. Transcripts levels of genes involved in contractility for FLNC-mutants. (A)** Heatmap plots showed downregulation of differentially expressed genes involved in cardiac contractility in FLNC mutant lines compared to control iPSC-CMs. **(B)** The FLNC<sup>G2189V61X</sup> line had lower *MYH7/MYH6* and FLNC<sup>E1891X</sup> line had higher *MYH7/MYH6* ratio compared to control. **(C)** The ratio of *TNNI3/TNNI1* were not significantly difference for both patients' lines compared to control iPSC-CMs. **(D)** Reduced number of FLNC<sup>G189V61X</sup> and FLNC<sup>E2189X</sup> transcripts were mapped to FLNC locus compared to controls as analyzed by IGV. **(E)** Quantitative representation of Transcript counts of control vs FLNC mutants.



**Fig. S3. Pluripotent stem cell markers and genotypes of FLNC knock out iPSC lines. (A)** Immunofluorescence staining against pluripotent stem cell markers of FLNC knockout iPSC lines. **(B)** Sanger sequencing confirmation of FLNC<sup>KO+/-</sup> and FLNC<sup>KO-/-</sup> knockout.



**Fig. S4. The effect of FLNC ablation in cardiomyocyte contraction. (A)** RNA-seq analysis indicated downregulation of pathways involved in cardiac contractility, sarcomere formation and ion transport at the cell membrane. **(B)** Heatmap plots showed downregulation of differentially expressed genes involved in cardiac contractility in FLNC knockout lines compared to isogenic control iPSC-CMs. **(C)** Validation of downregulation of sarcomeric genes transcripts in FLNC knockout lines compared to isogenic control iPSC-CMs by qPCR. **(D)** Irregular beating observed in FLNC homozygous knockout; pie chart shows percentage of arrhythmic cells in FLNC homozygous knockout iPSC-CMs.

**A****B****C****D**

**Fig. S5. FLNC interacts with CTNNB1. A)** Quantification of IP results. IP-FLNC: IP with FLNC antibody. IP-CTNNB1: IP with CTNNB1 antibody **B)** Geneset enrichment analysis using Molecular Signature Database: HALLMARK\_WNT\_BETA\_CATENIN\_SIGNALING showed similar trend as the  $\beta$ -catenin signaling geneset cataloged in DAVID.

# JW-67

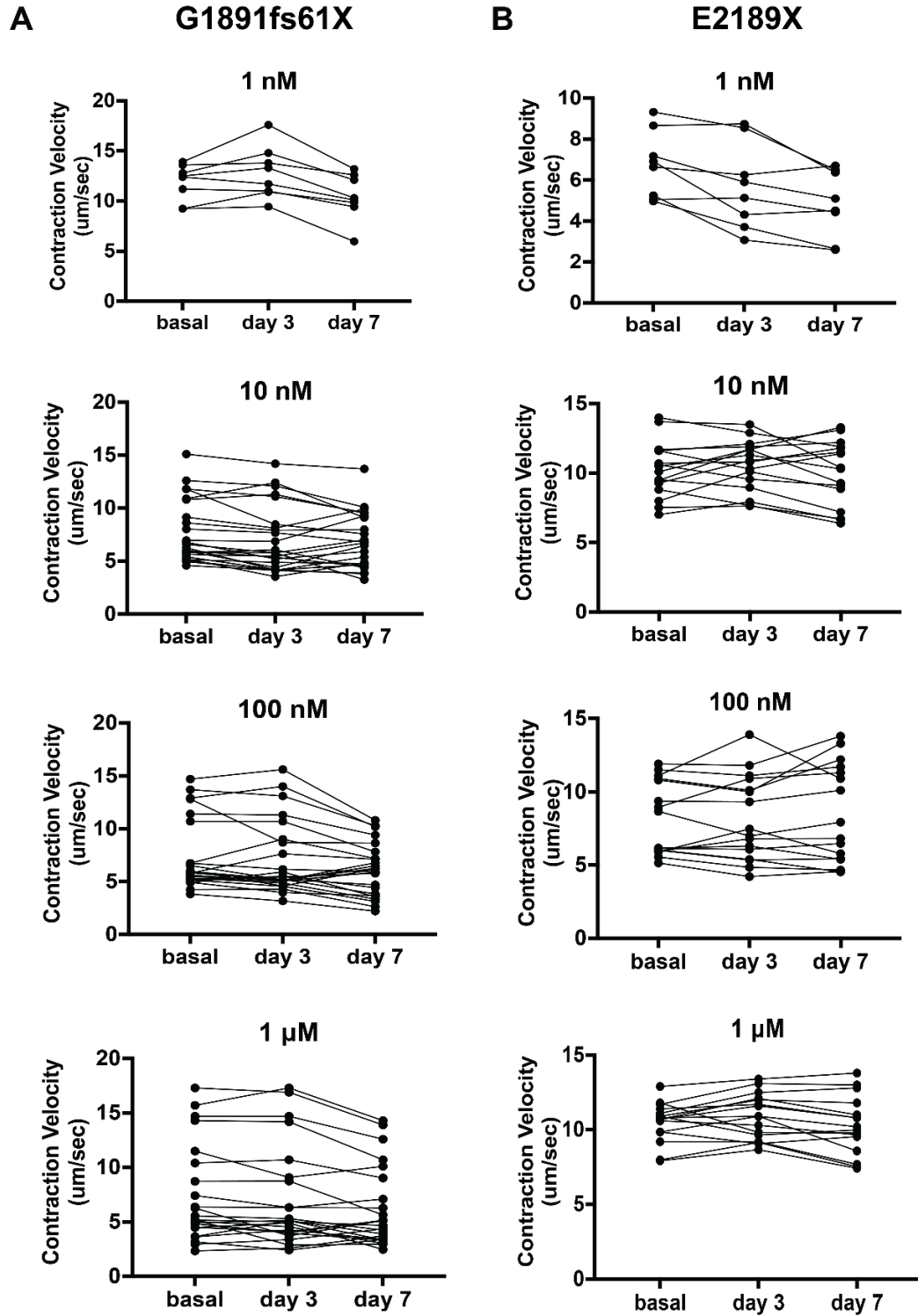


**Fig. S6. Lack of rescuing effect of JW-67 (Wnt inhibitor) on FLNC iPSC-CM contractility. Repeated measurement over the course of 7-days treatment.**

# JW-74

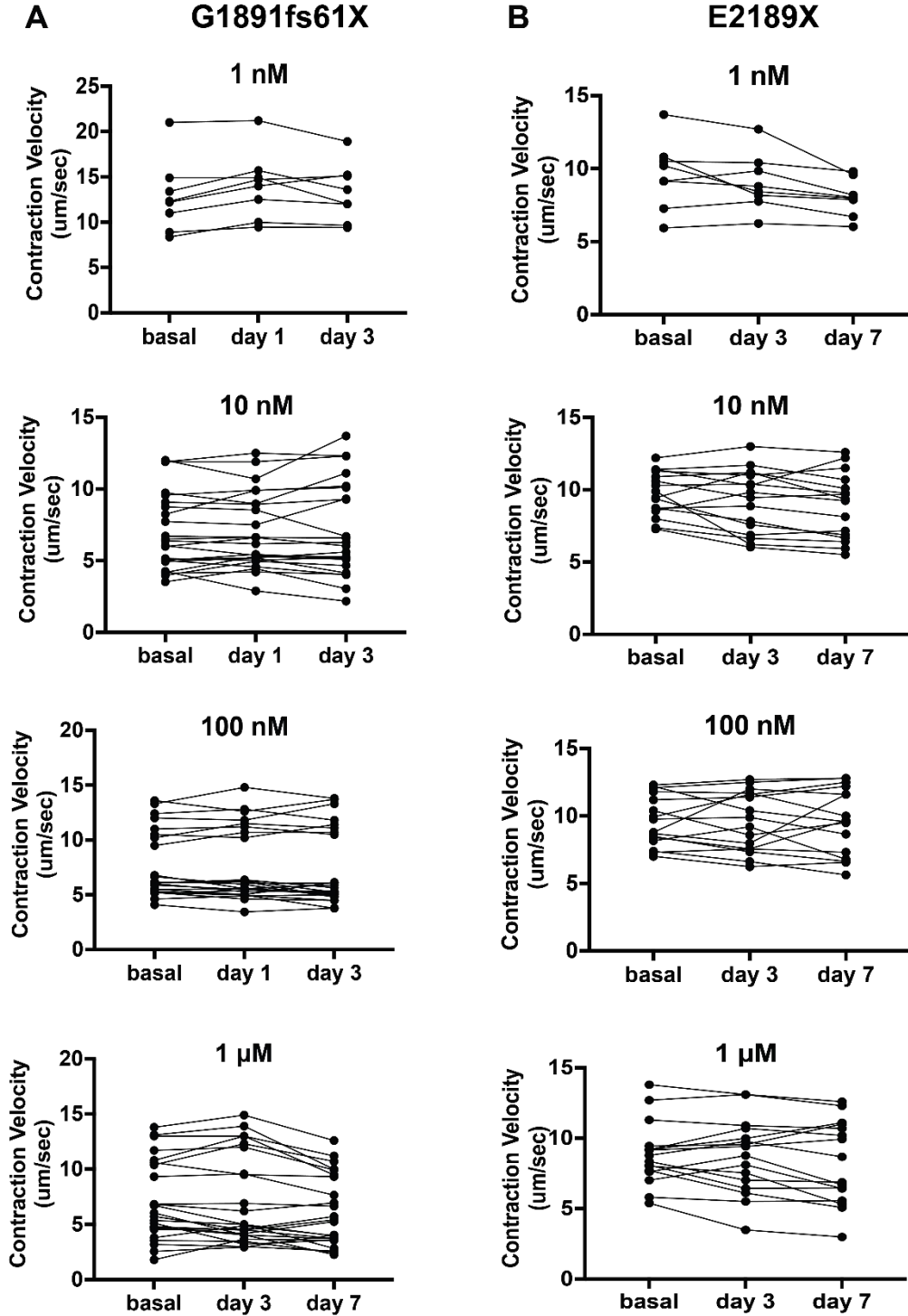


**Fig. S7.** Lack of rescuing effect of JW-74 (Wnt inhibitor) on FLNC iPSC-CM contractility. Repeated measurement over the course of 7-days treatment.

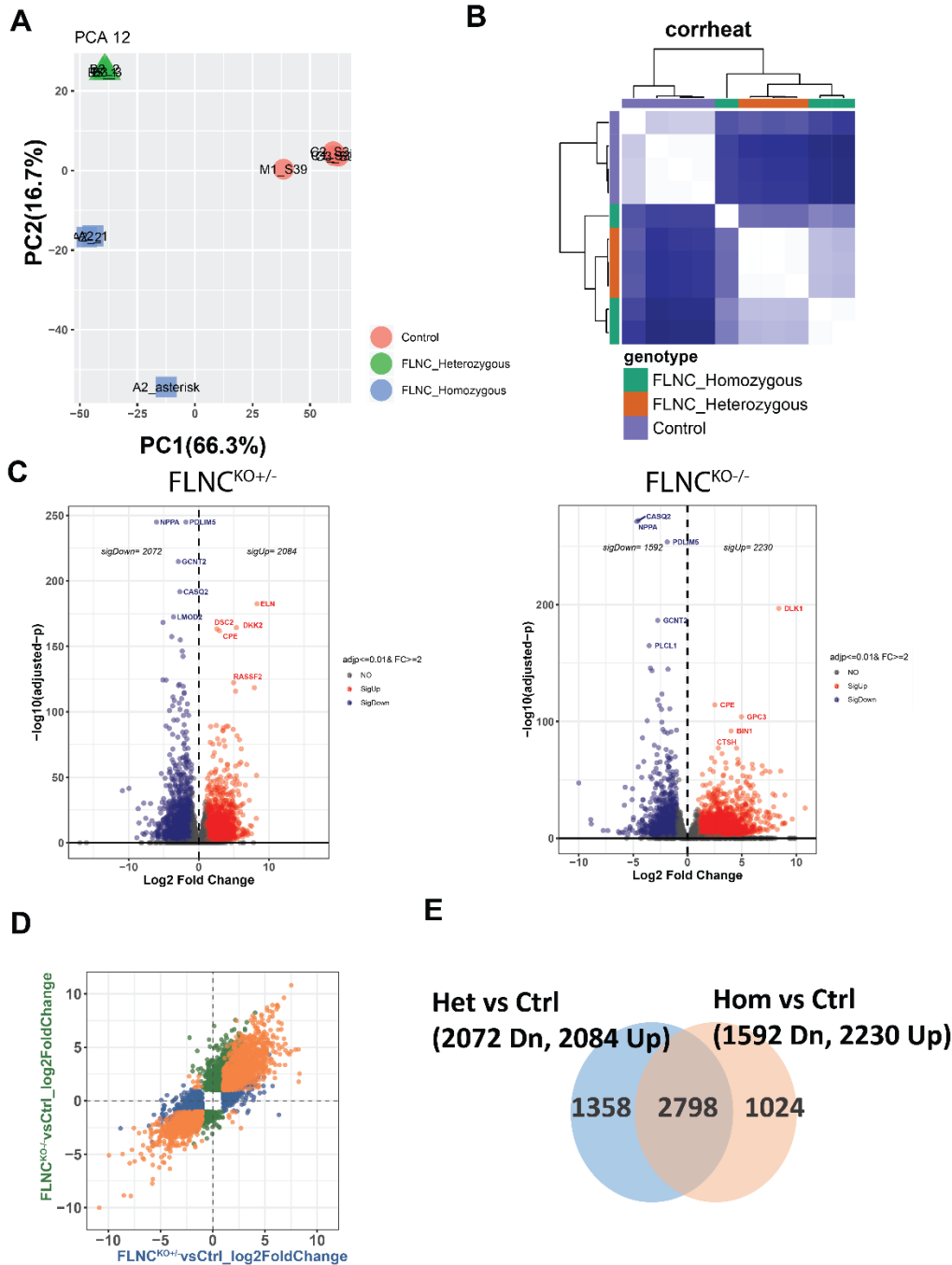


**Fig. S8. Dysregulated differentially expressed genes in FLNC heterozygous were highly concordant with homozygous iPSC-CMs.** (A) Principle component analysis indicated differentially expressed genes from FLNC heterozygous and homozygous varied greatly from isogenic control iPSC-CMs. (B) Heatmap plots of the DEGs from FLNC heterozygous and homozygous confirmed PCA analysis in (A). (C) Volcano plots of the upregulated and downregulated DEGs in FLNC heterozygous and homozygous iPSC-CMs. (D) Correlation analysis showed DEGs from FLNC heterozygous were highly concordant with DEGs from FLNC homozygous. (E) Venn diagram shows the number of DEGs shared between FLNC heterozygous and FLNC homozygous knockout.

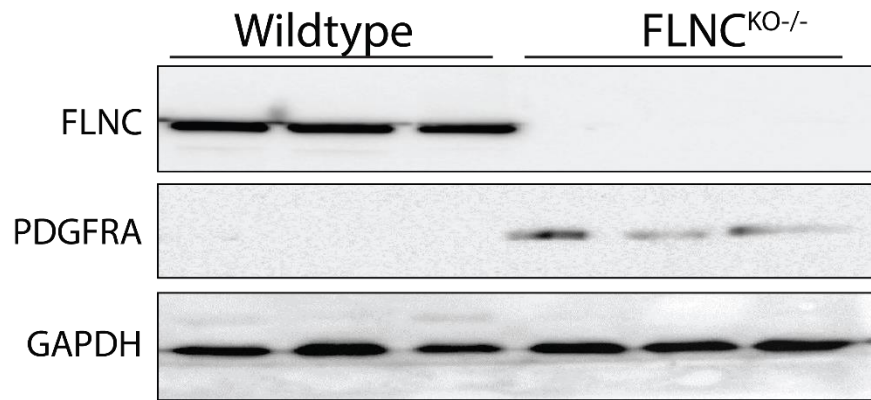


**Fig. S9. Upregulation of PDGFRA expression levels in FLNC<sup>KO/-</sup> clone #2.**

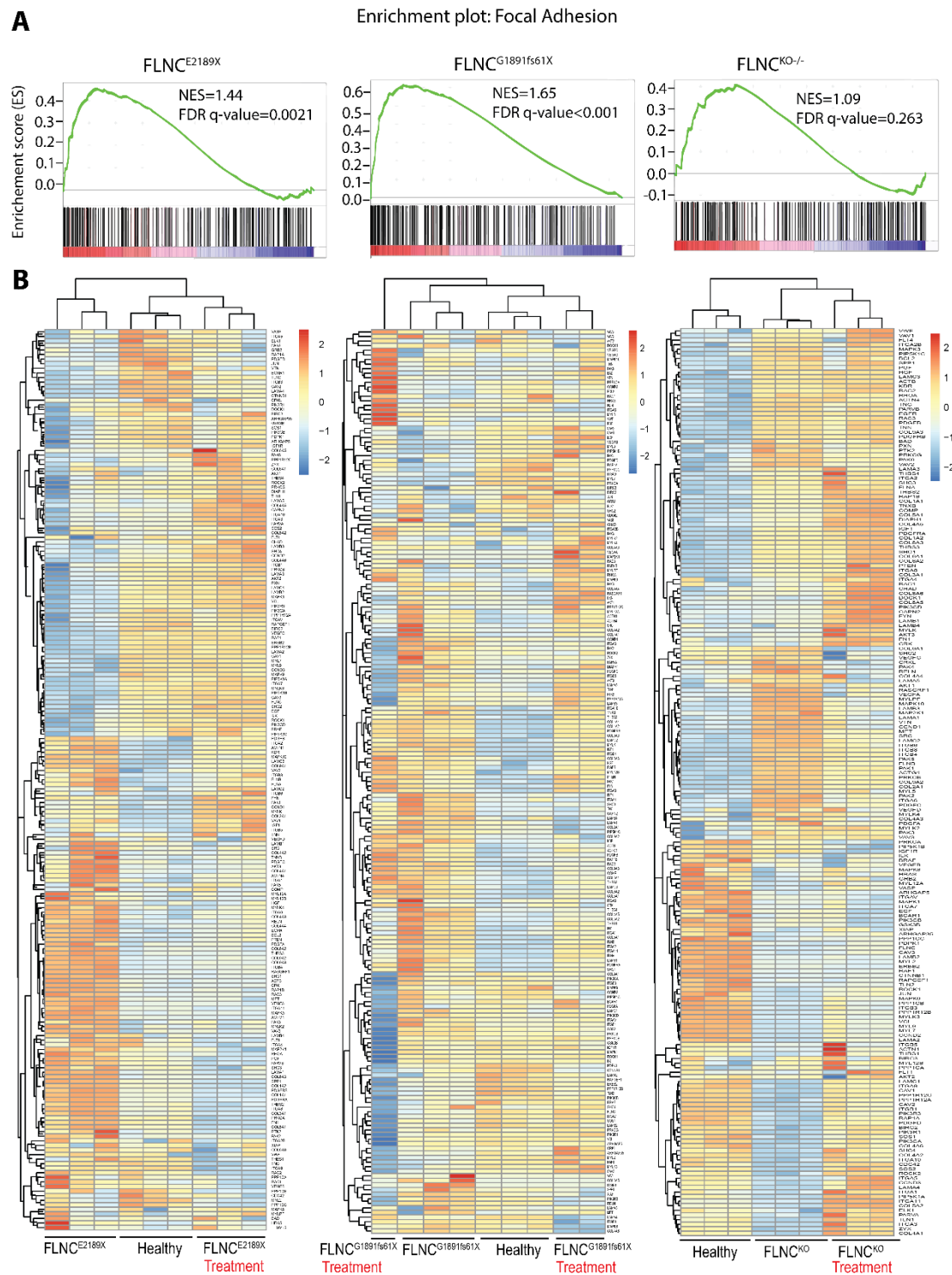
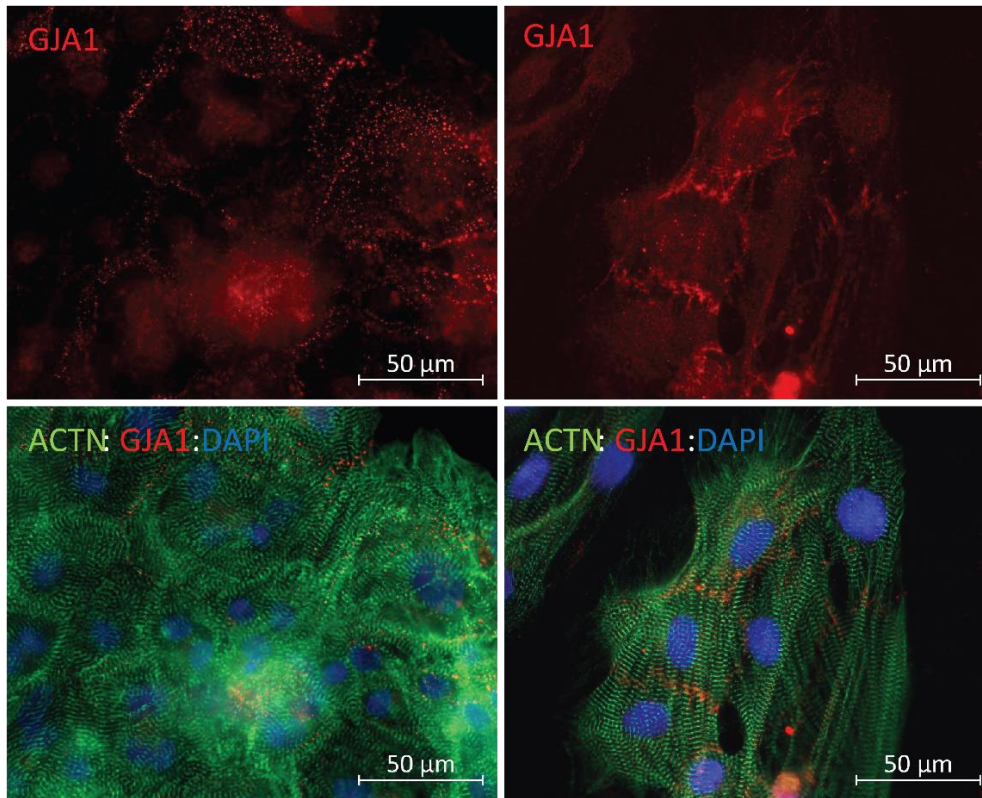


**Fig. S10. RNA-seq analysis showed dysregulation of cell-cell adhesion pathway. (A)** Cell adhesion pathway (hsa04510) was upregulated in FLNCE<sup>2189X</sup>, FLNCG<sup>1891V61X</sup> and FLNCKO<sup>-/-</sup>. **(B)** Heatmap of Differentially expressed gene of focal adhesion pathway in FLNCE<sup>2189X</sup>, FLNCG<sup>1891V61X</sup> and FLNCKO<sup>-/-</sup> iPSC-CMs complemented finding from (A).

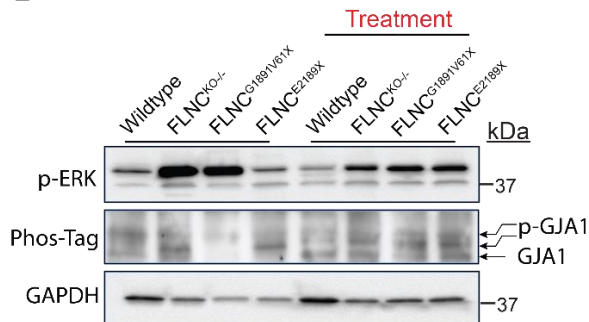
A

Healthy

Treatment



B



C

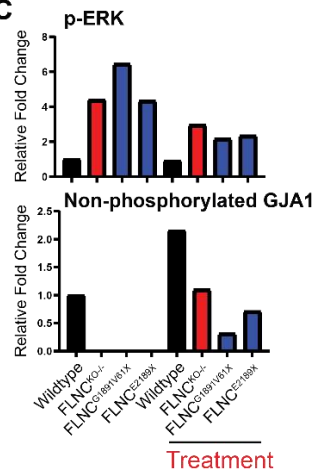


**Fig. S11. Immunofluorescence staining of GJA1 in healthy control after treatment with Crenolanib showed GJA1 localization to the plasma membrane. (A)** GJA1 localization to the plasma membrane. **(B)** The expression levels of phosphorylated-GJA1 (p-GJA1) were increased in FLNC patient-derived lines compared to healthy control iPSC-CMs and non-phosphorylated GJA1 was not detected in the FLNC-mutants iPSC-CMs. Upon PDGFRA inhibition, the expression levels of unphosphorylated GJA1 were increased in FLNC patient-derived iPSC-CMs. **(C)** Quantitative representative of the immunoblots in (B).

# Crenolanib

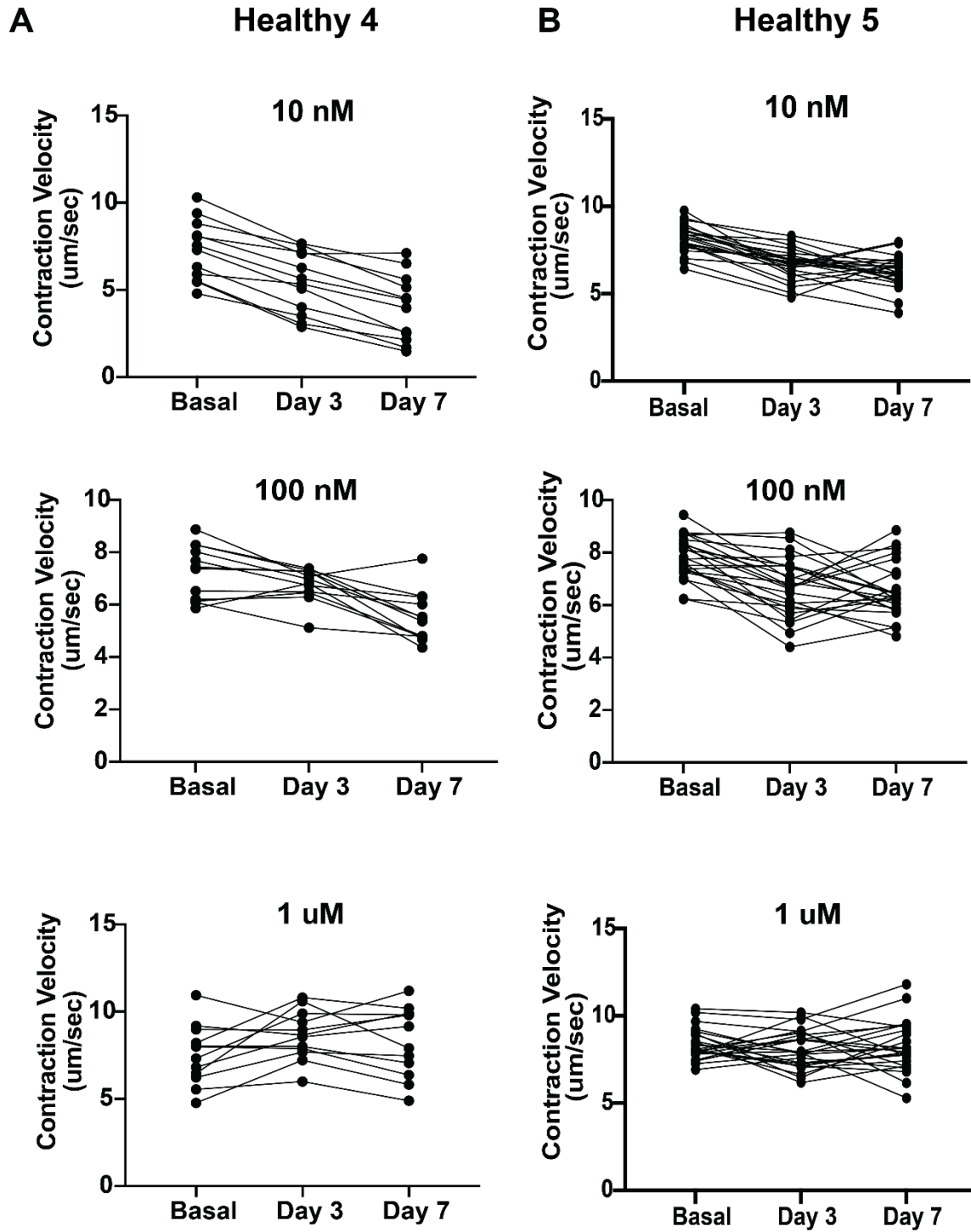


**Fig. S12. Lack of enhancement of crenolanib on healthy iPSC-CM contractility.** Repeated measurement over the course of 7-days treatment.

# Crenolanib

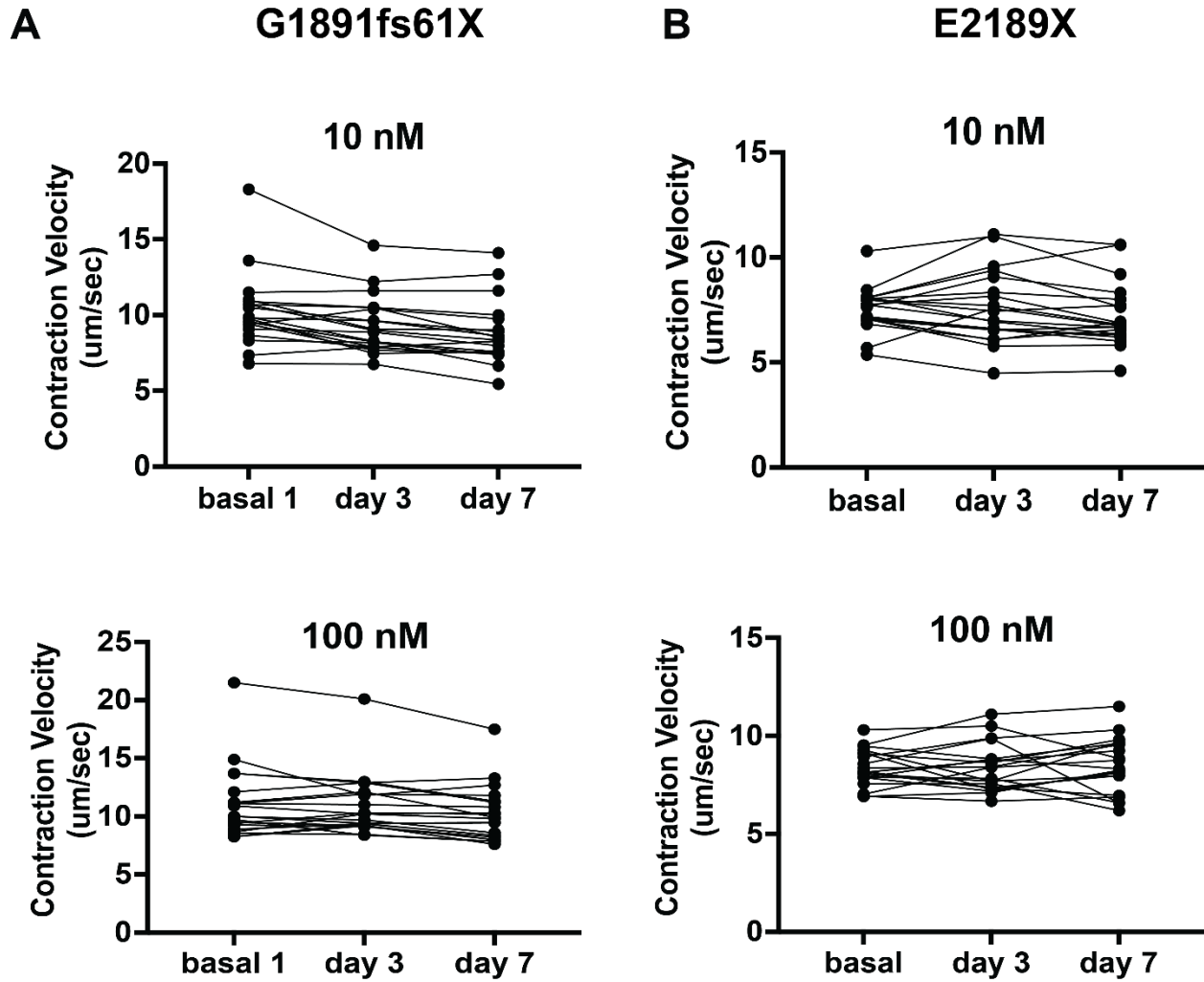


**Fig. S13. Dose response of crenolanib on FLNC iPSC-CM contractility.** Significant improvement was observed at 1  $\mu$ M (Fig. 6E). Repeated measurement over the course of 7-days treatment.

# LY3214996 Erk inhibitor

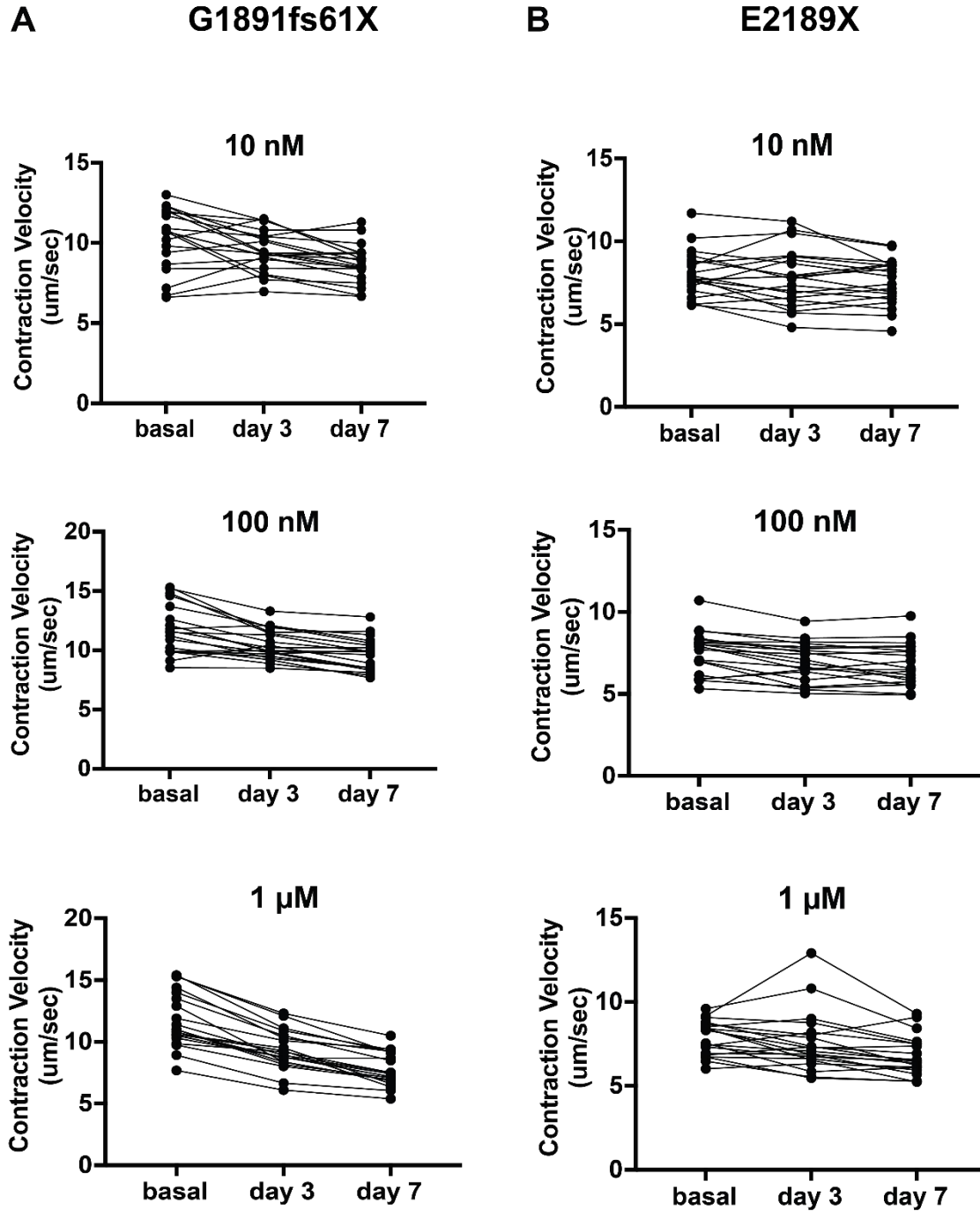


Fig. S14. Lack of rescuing effect of LY3214996 (Erk inhibitor) on FLNC iPSC-CM contractility. Repeated measurement over the course of 7-days treatment.

# Ulixertinib ERK inhibitor

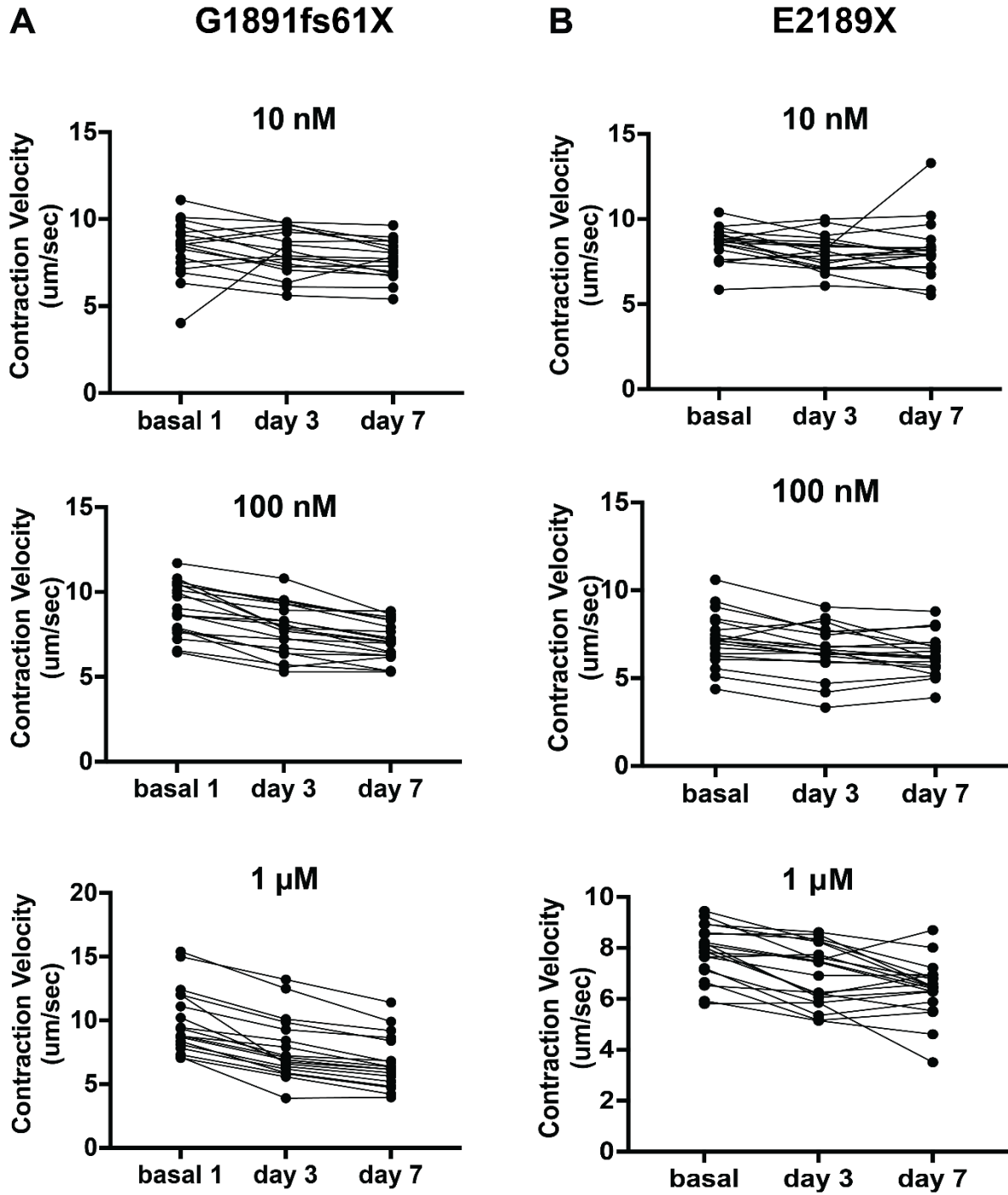
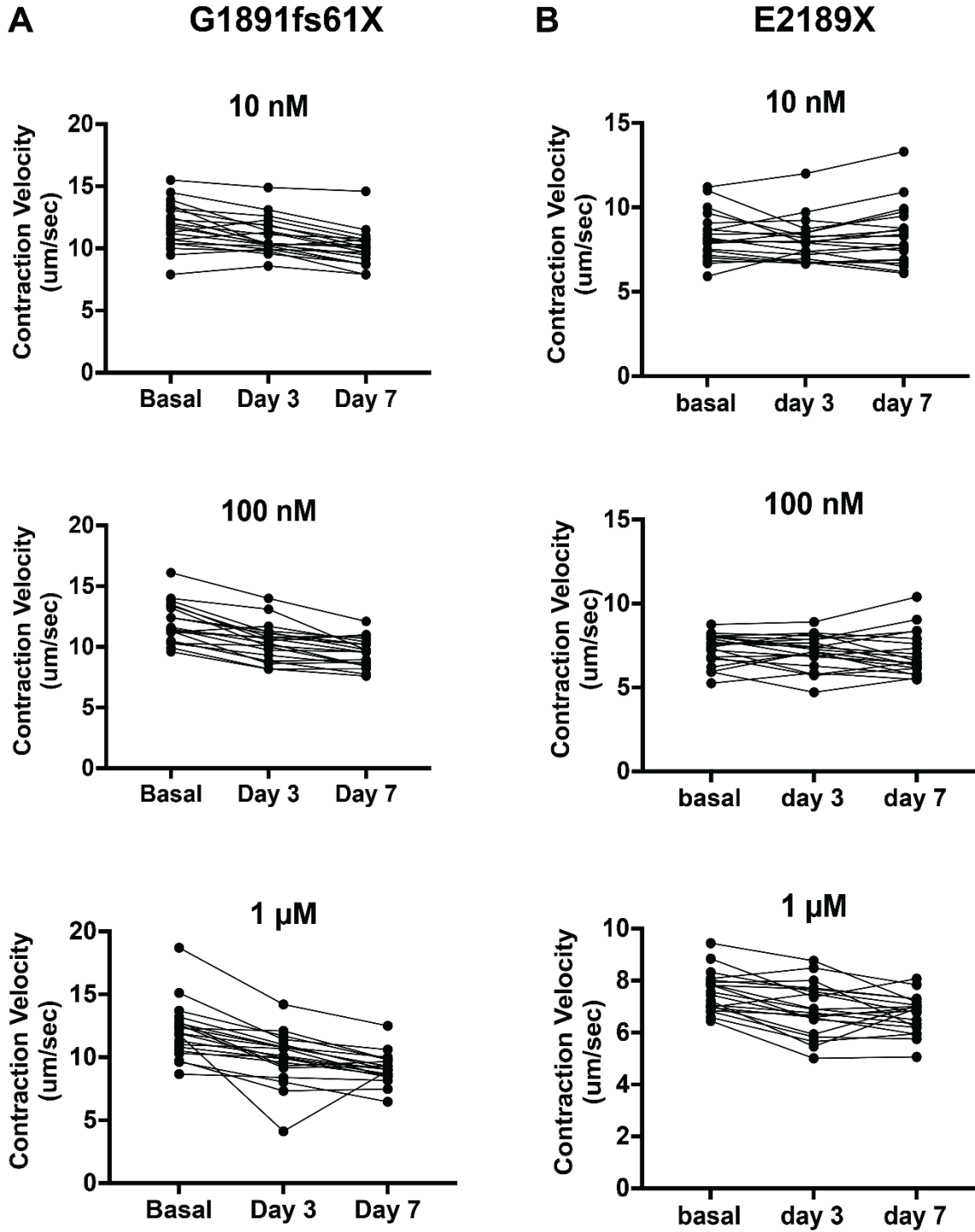


Fig. S15. Lack of rescuing effect of Ulixertinib (Erk inhibitor) on FLNC iPSC-CM contractility. Repeated measurement over the course of 7-days treatment.

# Adavosertib Wee1 inhibitor



**Fig. S16. Lack of rescuing effect of Adavosertib (Wee1 inhibitor) on FLNC iPSC-CM contractility. Repeated measurement over the course of 7-days treatment.**

# Cabozantinib

## Multiple receptor tyrosine kinase inhibitor

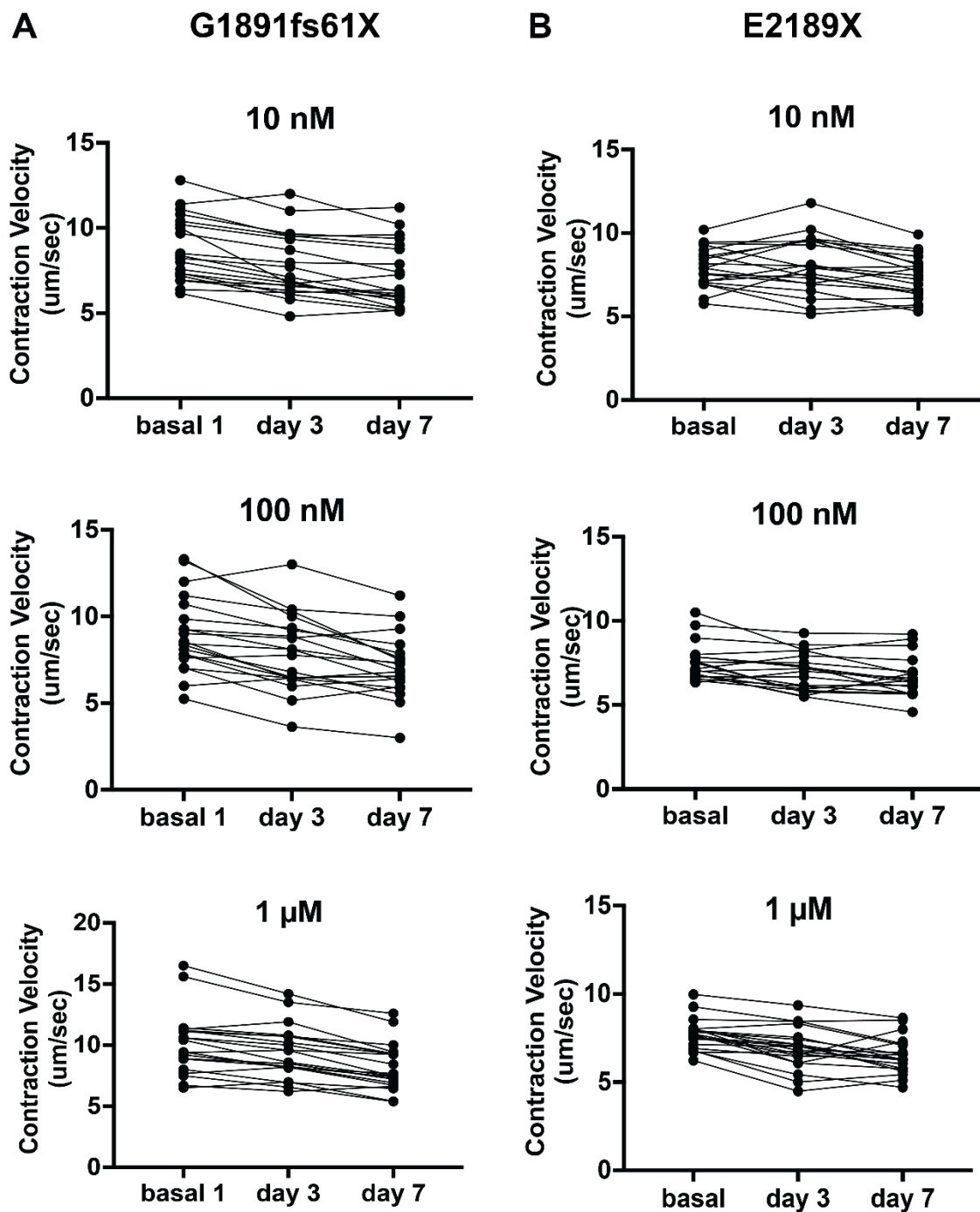
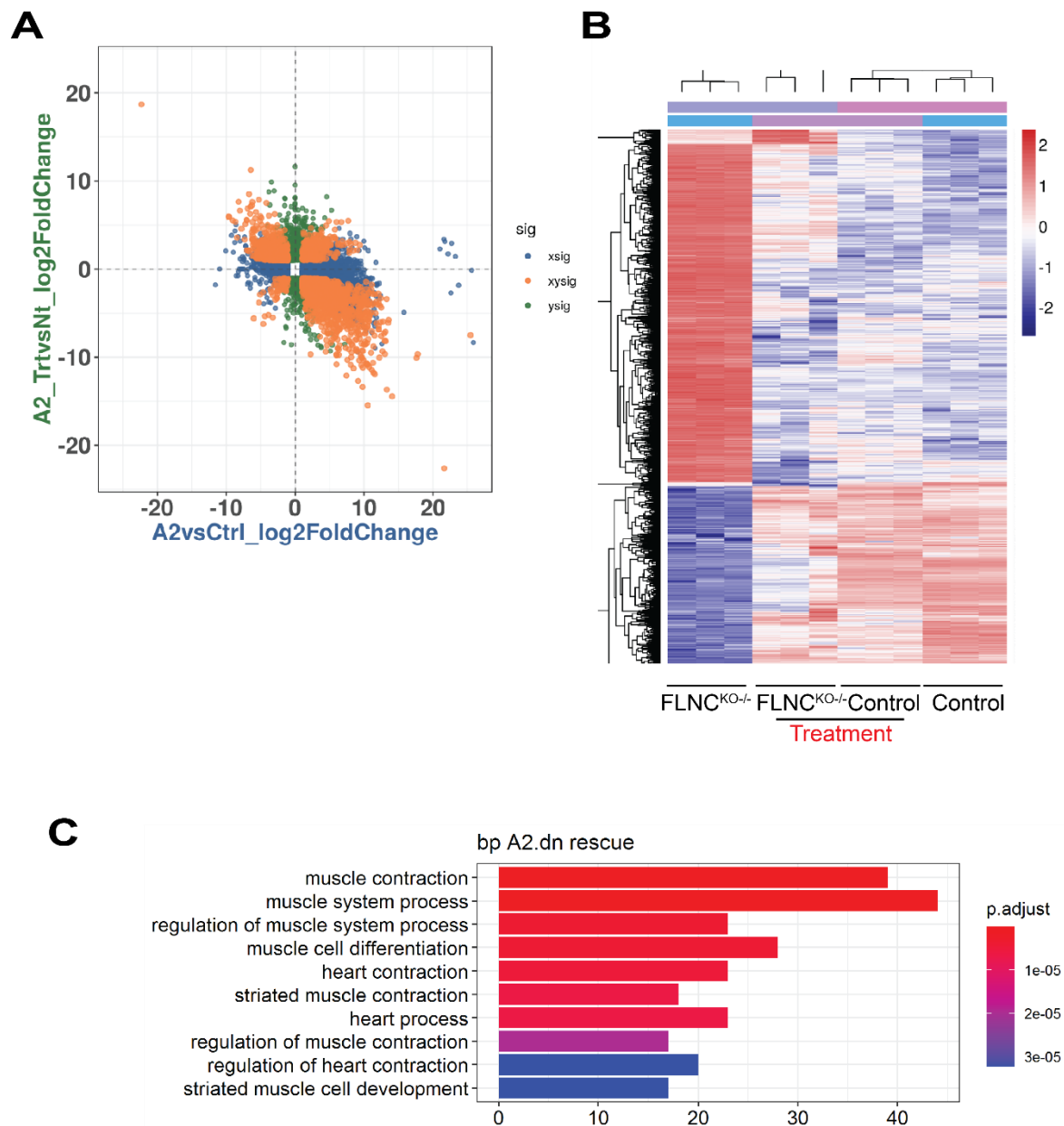
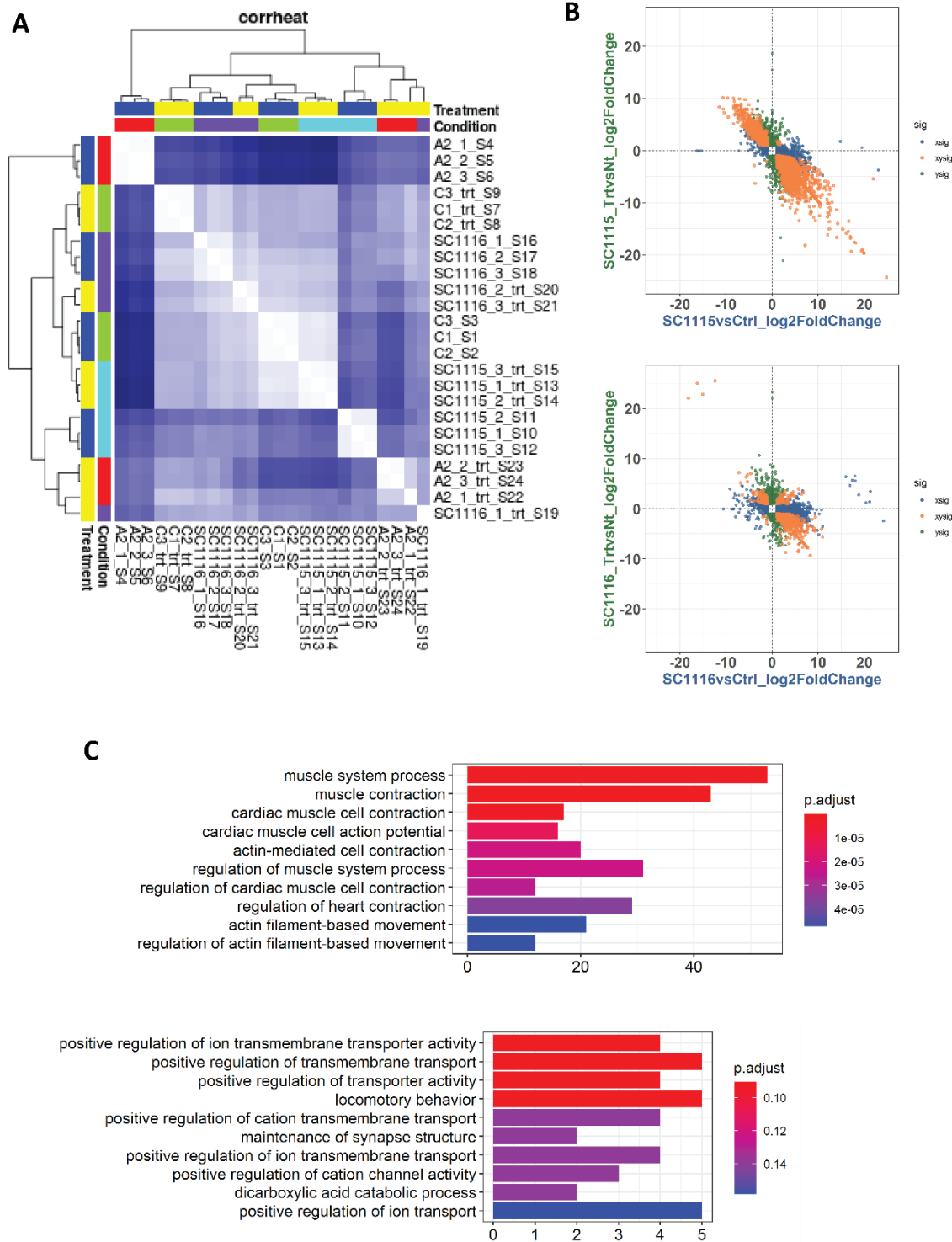


Fig. S17. Lack of rescuing effect of Cabozantinib (multiple receptor tyrosine kinase inhibitor) on FLNC iPSC-CM contractility. Repeated measurement over the course of 7-days treatment.



**Fig. S18. Partial normalization of DEGs in FLNC knockout iPSC-CMs. (A)** Correlation analysis showed that majority of the dysregulated genes in FLNC homozygous knockout iPSC-CMs were reverted after treatment. **(B)** Heatmap of DEGs evidenced the correlation analysis on DEGs from FLNC<sup>KO/-</sup> iPSC-CMs after treatment. Specifically, 901 DEGs were downregulated after treatment (941 were upregulated before treatment) and 510 DEGs were upregulated after treatment (520 DEGs were downregulated before treatment).



**Fig. S19. Partial normalization of DEGs in patients and FLNC knockout iPSC-CMs. (A)** heatmap plots of DEGs before and after treatment in FLNC mutant lines compared to control iPSC-CMs. **(B)** Correlation analysis showed inversed relationship of the DEGs from FLNC<sup>G1891V61X</sup> and FLNC<sup>E2189X</sup> before and after treatment with crenolanib. **(C)** RNA-seq analysis showed partial rescue of pathways involved in cardiac contractility of cardiac myocytes.



**Table 1. List of Antibodies for Immunoblotting.**

Antibodies	Vendor	Dilution
Active $\beta$ catenin	Millipore (05-665)	1:1000
Connexin 43	SIGMA <sup>®</sup> (C6219)	1:5000
Plakoglobin	SIGMA <sup>®</sup> (P8087)	1:1000
Desmoplakin	Abcam (ab109445)	1:1000
ERK1/2	Cell Signaling (9102)	1:1000
Phospho-ERK1/2	Cell Signaling (4370)	1:1000
FLNC	Atlas (HPA006135)	1:1000
GAPDH	Abcam (ab9485)	1:5000

**Table 2. List of Antibodies for Immunofluorescence.**

Antibodies	Vendor	Dilution
Sarcomeric alpha actinin	Abcam (ab9465)	1:500
Connexin 43	SIGMA <sup>®</sup> (C6219)	1:1000
Active $\beta$ catenin	Active $\beta$ catenin (05-665)	1:500
FLNC	Atlas (HPA006135)	1:250
PCM1	SIGMA (HPA023370)	1:250

**Table 3. List of Primers for qPCR.**

Gene	Primer Sequence
FLNC	Forward: CCTATGCTGTTCTCCATGTG Reverse: TAGATGTCAAAGTAGGTGGG
GATA4	Forward: ATAAATCTAAGACACCAGCAG Reverse: CCGTAGTGAGATGACAGG
MYH6	Forward: AGCAGAGAACTTTGACAAG Reverse: TCCTGAAGGTTCTTGTTCTC

MYH7	Forward: GGATGAGGAGGAGATGAATG Reverse: TTTCACCTTGTTCTCTGTTG
RYR2	Forward: CGTGCGTATCTTAGCTATTC Reverse: GGACTTTCAAGCAGTAGTATC
GAPDH	Forward: CTTTTGCGTCGCCAG Reverse: TTGATGGCAACAATATCCAC
MYC	Forward: TGAGGAGGAACAAGAAGATG Reverse: ATCCAGACTCTGACCTTTTG
TGFB3	Forward: TGTTGAGAAGAGAGTCCAAC Reverse: ATCACCTCGTGAATGTTTTTC
TCF4	Forward: CAGATGTAAAAGGGTCCAAG Reverse: AAATGGGGGTTAAGGAGAAG
SOX9	Forward: CTCTGGAGACTTCTGAACG Reverse: AGATGTGCGTCTGCTC
COL1A2	Forward: GTGGTTACTACTGGATTGAC Reverse: CTGCCAGCATTGATAGTTTC
PDGFRA	Forward: TGCTGGAAGAAATCAAAGTC Reverse: CTCATGGACAGAAATAGTGAC
AKT3	Forward: TTCTTCTCTGGAGTAAACTGG Reverse: TTGCTGACATTTTTTCAGGTG
CCND1	Forward: GCCTCTAAGATGAAGGAGAC Reverse: CCATTTGCAGCAGCTC
AXIN2	Forward: AAAGAGAGGAGGTTTCAGATG Reverse: CTGAGTCTGGGAATTTTTCTTC
CD44	Forward: TTATCAGGGACCAAGACAC Reverse: ATCAGCCATTCTGGAATTTG
CDH1	Forward: CCGAGAGCTACACGTTTC

	Reverse:TCTTCAAATTCACCTCTGCC
PAX3	Forward:ATCAACTGATGGCTTTCAAC Reverse:CAGCTTGTGGAATAGATGTG